Compressive strengths of molybdenum alloy micro-pillars prepared using a new technique

H. Bei,[a,b,*] S. Shim,[a,b] E.P. George,[a,b] M.K. Miller,[b] E.G. Herbert[c] and G.M. Pharr[a,b]

[a]Department of Materials Science and Engineering, The University of Tennessee, Knoxville, TN 37996, USA
[b]Materials Science and Technology Division, Oak Ridge National Laboratory, Oak Ridge, TN 37831, USA
[c]MTS Nano Instruments Innovation Center, Oak Ridge, TN 37830, USA

Single-crystal micro-pillars of a molybdenum alloy were prepared by a new technique that involves chemically etching away the matrix of a directionally solidified NiAl–Mo eutectic. The square cross-section pillars had edge dimensions ranging from ∼360 to ∼1000 nm. When tested in compression with a nanoindentation system, the pillars all yielded, regardless of size, at a critical resolved shear stress of 4.3 GPa, or $G/26$, where G is the shear modulus. This shear yield strength is in the range expected for the theoretical strength, $G/30$ to $G/10$.
© 2007 Acta Materialia Inc. Published by Elsevier Ltd. All rights reserved.

Numerous studies over the past decade have shown that the strength of metals and alloys, when measured at small scales, can be considerably greater than that determined in more conventional macroscopic tests. In some cases, this enhanced strength results from the unusual ways the material must be tested due to the small specimen size. For example, nanoindentation hardness measurement of thin films can be accomplished only with the film attached to a substrate, and when the substrate is hard and rigid, the film can appear to be much harder than it actually is [1,2]. For convenience, tensile testing of thin films is also sometimes conducted with the film attached to a substrate, in which case the yield strength can be much higher than for a free-standing film [3,4]. Strength can also increase when the testing method imposes plastic strain gradients – a phenomenon that has been explained in terms of size-dependent strengthening mechanisms caused by geometrically necessary dislocations [5,6]. Strain gradient effects have been well documented in nanoindentation [7–9], micro-torsion [10] and micro-bend experiments [11], and become measurable only when the sample size is small, typically of the order of a few micrometers.

In order to avoid the complications arising from substrate influences and strain gradient effects, small-scale compression testing of micro-pillars has recently been employed to explore other important aspects of small-scale plasticity [12–22]. Since strain gradients are minimized in compression testing, strengthening due to other factors, such as finite numbers of dislocations in the sample volume and the interaction of dislocations with nearby free surfaces, can be examined. Such tests have been greatly facilitated by advances in focused ion beam (FIB) technology, which has been used to mill small cylindrical pillars with dimensions of a micrometer or less from materials such as Ni, Au, Al and Ni₃Al [12–20]. To date, micro-pillar tests on single-phase metals have generally shown a distinct size effect, with the yield and flow strength increasing with decreasing pillar diameter [12–20]. Curiously, however, there have been no observations of strengths near the theoretical, even though some of the pillar diameters are small enough that they would be expected to contain vanishingly small dislocation populations. For example, for a typical dislocation density of $10^{12} \, \text{m}^{-2}$, the average dislocation spacing is 1 μm, so there is a reasonable chance that a specimen with micrometer dimensions would be dislocation free, and yielding would require the nucleation of dislocations at stresses near the theoretical strength [23].

A summary of micro-pillar observations is given in Table 1, which demonstrates that the shear flow stresses

---

* Corresponding author. Address: Materials Science and Technology Division, Oak Ridge National Laboratory, 1 Bethel Valley Road, Oak Ridge, TN 37831, USA. Tel.: +1 865 5744343; fax: +1 865 5747659; e-mail: Beih@ornl.gov

observed to date are not much greater than $G/100$, where G is the shear modulus. This is considerably smaller than the theoretical shear strength, which is normally estimated to be in the range $G/30$ to $G/10$ [24,25]. In addition, the strengths listed in Table 1 are the highest flow stresses observed in the tests, with yield strengths frequently being much lower. These observations are especially perplexing when compared to the now classic tensile tests on small metallic whiskers 1–15 μm in diameter conducted by Brenner 50 years ago [24,26], in which shear yield strengths of $G/30$ or greater were achieved (results included in Table 1).

A possible explanation for the low yield and flow stresses in micro-pillar tests is that strength-degrading surface defects are introduced during FIB milling by the high-energy Ga ions (usually 30 keV) [27]. Defect production, including recent observations of near surface dislocations [28], amorphization and mixing of materials after ion beam exposure, have all been observed during the preparation of transmission electron microscope (TEM) samples by FIB methods [27,28]. For this reason, other techniques for micro-pillar specimen preparation have been sought, but none has yet produced a strength near the theoretical [17,18,21].

Here, we report on micro-pillars produced in a new way that avoids the complications of FIB-related defects and damage. The shear yield strength of the pillars is $\sim G/26$, which, in combination with several other aspects of the observed deformation behavior, suggests that the pillars do indeed deform at the theoretical strength.

The micro-pillars were produced by etching away the NiAl matrix of a NiAl–Mo in situ composite grown by directional solidification (Fig. 1). Details of the directional solidification process and the resulting composite microstructures have been discussed elsewhere [29]. The composite consists of monocrystalline Mo solid-solution fibers (composition, 86Mo–10Al–4Ni, at.%) with axes parallel to $\langle 100 \rangle$ embedded in a NiAl matrix (composition, 55Ni–45Al, at.%) [29]. The cross-sectional area (A) of the fibers, which varies inversely as the directional solidification rate, was measured from scanning electron microscope (SEM) images using image-analysis software. Because of their nearly square cross-sections (Fig. 1a), the fiber (or pillar) size (a) is taken to be the square root of the measured cross-sectional area. The pillar sizes in this study ranged from 360 to 1000 nm.

Compression testing was performed in a nanoindentation system with flat punch diamond indenters ion milled to circular cross sections with diameters of 0.8 and 2.2 μm. Rather than identify and locate individual pillars for testing, the nanoindenter was programmed to make an array of tests at 144 locations on each specimen – a 12×12 array spaced 5 μm apart – while measuring the load (P) and displacement (h). With this method, the indenter was accurately positioned over the centers of a few individual pillars, as shown in Figure 1d. However, many tests completely missed the pillar, compressed adjacent pillars simultaneously (arrow in Fig. 1b), or compressed only part of a pillar (Fig. 1c), thereby invalidating the measurement.

Examples of P–h curves obtained from good compression tests on the four different size pillars are shown in Figure 2a. The reproducible P–h curves are initially linear elastic but, upon reaching a critical load, there is

Table 1. Summary of maximum strengths observed in compression testing of micro-pillars and tensile testing of small whiskers (compressive or tensile strength, σ; resolved shear strength, τ)

Material	Largest observed stress		Sample size [μm]	G (GPa)	Normalized stress		Ref.
	σ (GPa)	τ (GPa)			σ/G	τ/G	
Pillars (compression)							
Nanocrystalline Ni	1.498[a]	0.749[b]	20	78	0.019	0.010	[21]
Single crystal Au	0.56[c]	0.27[d]	0.18	27	0.021	0.010	[19]
Single crystal Au	0.55[e]	0.275[b]	0.4	27	0.020	0.010	[17]
Single crystal Ni	–	0.25[f]	1	78	–	0.003	[14]
Single crystal Ni	0.125[g]	0.063[b]	5	78	0.002	0.001	[12]
Ni₃Al–1% Ta	2[g]	1[b]	0.5	70	0.029	0.014	[12]
UM-F19 (Ni superalloy)	1.45[h]	0.725[b]	1.8	60	0.024	0.012	[13]
Ni₃Al	1.174[a]	0.587[b]	2	70	0.017	0.008	[22]
Whiskers (tension)							
Fe	–	3.587	1.6	59.8	–	0.06	[24]
Cu	–	0.798	1.25	36.3	–	0.022	[24]
Ag	–	6.987	3.8	22.5	–	0.031	[24]
Mo pillars (compression)							
Mo–10Al–4–Ni	10.36[g]	4.87[i]	0.36–1	111.5	0.093	0.044	This study

The strengths are flow stresses at various levels of strain, with yield strengths often being much smaller.
[a] 2% offset stress.
[b] Schmid factor of 0.5 is assumed.
[c] Flow stress at 5% plastic strain.
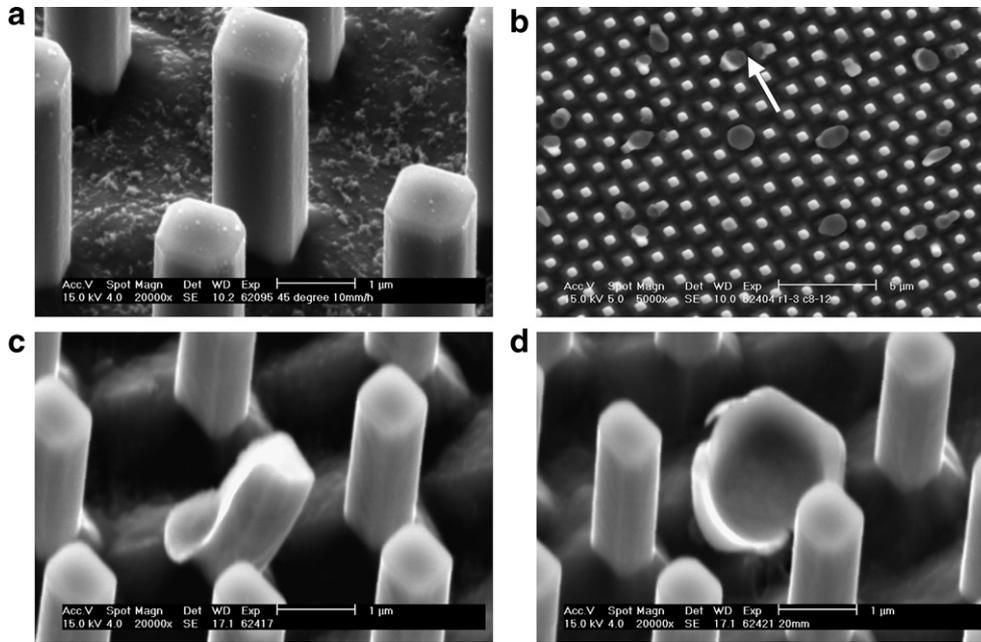[d] Schmid factor of 0.48 used.
[e] Flow stress at 10% plastic strain.
[f] Shear stress at 1% plastic strain.
[g] Yield strength.
[h] Flow stress at 3% plastic strain.
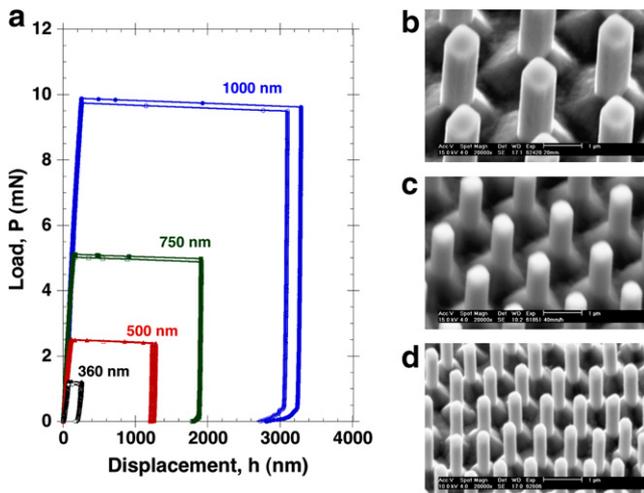[i] Schmid factor of 0.47 is used.

Figure 1. Molybdenum alloy micro-pillars fabricated by selective etching of the matrix in a NiAl–Mo directionally solidified eutectic: (a) as-fabricated pillars with a nominal edge dimension of 1 μm; (b) a region chosen for compression testing illustrating alignment of the cylindrical diamond punch with the pillars (the arrow points to two pillars that were contacted simultaneously, invalidating the test); (c) a pillar that was not squarely contacted; and (d) a pillar that was squarely contacted to give a valid test.

a sudden displacement burst (pop-in) corresponding to plastic yielding, and the pillars undergo severe plastic deformation and flattening (Fig. 1d). The magnitude of the displacement burst corresponds well to the height of the pillar (the pillars had aspect ratios in the range 2.5–3.0), confirming that once plasticity commences, it continues catastrophically and unstably until the pillar is fully compressed. Since the tests were conducted in load control at a constant loading rate, the instability suggests that there is significant strain softening after yielding, as was observed by Brenner in his micro-whis-ker tests [24,26]. Quantification of the strain softening behavior would require a displacement-controlled test.

Yield strengths for the valid tests computed from measured loads at yielding and initial cross-sectional areas are summarized in Table 2. Curiously, the average yield strength is independent of pillar size at a value near 9.2 GPa. The slip systems in Mo are $(110)[1\bar{1}1]$ and $(112)[11\bar{1}]$ [30], which for our compression geometry yields Schmid factors of 0.41 and 0.47. Assuming that slip occurs on the slip system with the higher Schmid factor, the critical resolved shear stress at yielding is $\tau_r = 4.3$ GPa. The shear modulus of Mo is 126 GPa [31], but assuming that alloying with Al and Ni lowers this according to a rule of mixtures based on their respective atomic percentages, G for our micro-pillars should be approximately 112 GPa. Thus, the measured resolved shear stress at yielding is approximately $G/26$ and therefore within the range expected for the theoretical strength ($G/30$ to $G/10$) [24,25]. This large critical resolved shear stress suggests that our micro-pillars are essentially dislocation-free before testing, consistent with transmission electron microscopy observations of NiAl–Mo eutectics [32], and that yielding occurs when

Figure 2. Micro-compression tests of molybdenum alloy pillars with sizes in the range 360–1000 nm: (a) compressive load–displacement curves; SEM images of micro-pillars with nominal edge dimensions of (b) 750 nm, (c) 500 nm and (d) 360 nm.

Table 2. Summary of compressive yield strengths obtained in this study for molybdenum alloy micro-pillars of various sizes

Nominal pillar size, a (μm)	Number of valid tests	Measured area, A (μm²)	Compressive yield strength (GPa)
1.00	5	1.00 ± 0.02	9.17 ± 0.44
0.75	4	0.58 ± 0.02	9.24 ± 0.77
0.50	12	0.26 ± 0.02	9.30 ± 0.48
0.36	9	0.13 ± 0.02[a]	9.18 ± 1.16

[a] Areas were not measured for individual tests but based on 36 randomly chosen pillars.

dislocations are nucleated at the theoretical shear strength, similar to Brenner's whisker tests. This conclusion is further corroborated by the fact that yield strength is independent of sample size. The fact that there is an intense burst of plasticity after yielding indicates that dislocation multiplication is rapid and widespread and that dislocation starvation does not occur in any of the specimens after yielding.

These results are consistent with the view that well-annealed metals, which have dislocation densities in the range $\sim 10^7$–10^{11} m^{-2} [33], should behave as ideal metals (i.e. have yield strengths approaching the theoretical strength) when their sizes are ~ 1 μm or smaller. It is surprising, therefore, that no other micro-pillar tests performed to date have observed such high yield stresses, even though some of the pillars were of appropriate dimensions (~ 1 μm or smaller). Possible reasons for the lower stresses measured in the previous studies include the generation of small dislocation loops and vacancies during FIB milling, and additional internal stresses from the implanted gallium ions due to the size difference between gallium and the host lattice. Although a size effect on yield stress was not observed in the present study, the current results do not rule out a size effect on the flow stress if stable deformation after yielding could be achieved through a displacement-controlled test.

[1] G.M. Pharr, W.C. Oliver, MRS Bull. 17 (1992) 28–33.
[2] T.Y. Tsui, G.M. Pharr, J. Mater. Res. 14 (1999) 292–301.
[3] W.D. Nix, Met. Trans. A 20 (1989) 2217–2245.
[4] O. Kraft, C.A. Volkert, Adv. Eng. Mater. 3 (2001) 99–110.
[5] M.F. Ashby, Philos. Mag. 21 (1970) 399–424.
[6] H. Gao, Y. Huang, W.D. Nix, J.W. Hutchinson, J. Mech. Phys. Solids 47 (1999) 1239–1263.
[7] K.W. McElhaney, J.J. Vlassak, W.D. Nix, J. Mater. Res. 13 (1998) 1300–1306.
[8] W.D. Nix, H.J. Gao, J. Mech. Phys. Solids 46 (1998) 411–425.
[9] J.G. Swadener, E.P. George, G.M. Pharr, J. Mech. Phys. Solids 50 (2002) 681–694.
[10] N.A. Fleck, G.M. Muller, M.F. Ashby, J.W. Hutchinson, Acta Metall. Mater. 42 (1994) 475–487.
[11] J.S. Stolken, A.G. Evans, Acta Mater. 46 (1998) 5109–5115.
[12] M.D. Uchic, D.M. Dimiduk, J.N. Florando, W.D. Nix, Science 305 (2004) 986–989.
[13] M.D. Uchic, D.M. Dimiduk, Mater. Sci. Eng. A 400 (2005) 268–278.
[14] D.M. Dimiduk, M.D. Uchic, T.A. Parthasarathy, Acta Mater. 53 (2005) 4065–4077.
[15] J.R. Greer, W.D. Nix, Appl. Phys. A 80 (2005) 1625–1629.
[16] J.R. Greer, W.C. Oliver, W.D. Nix, Acta Mater. 53 (2005) 1821–1830.
[17] J.R. Greer, W.C. Oliver, W.D. Nix, Acta Mater. 54 (2006) 1705.
[18] D.M. Dimiduk, C. Woodward, R. LeSar, M.D. Uchic, Science 312 (2006) 1188–1190.
[19] C.A. Volkert, E.T. Lilleodden, Philos. Mag. 86 (2006) 5567–5579.
[20] J.R. Greer, W.D. Nix, Phys. Rev. B 73 (2006) 245410.
[21] B.E. Schuster, Q. Wei, H. Zhang, K.T. Ramesh, Appl. Phys. Lett. 88 (2006) 103112.
[22] M.D. Uchic, M.A. Groeber, D.M. Dimiduk, J.P. Simmons, Scripta Mater. 55 (2006) 23–28.
[23] H. Bei, E.P. George, J.L. Hay, G.M. Pharr, Phys. Rev. Lett. 95 (2005) 045501.
[24] S.S. Brenner, J. Appl. Phys. 27 (1956) 1484–1956.
[25] A.H. Cottrell, Dislocations and Plastic Flow in Crystals, Clarendon Press, Oxford, 1953.
[26] S.S. Brenner, J. Appl. Phys. 28 (1957) 1023–1026.
[27] J.P. McCaffrey, M.W. Phaneuf, L.D. Madsen, Ultramicroscopy 87 (2001) 97–104.
[28] D. Kiener, C. Motz, M. Rester, M. Jenko, G. Dehm, Mater. Sci. Eng. A 459 (2007) 262–272.
[29] H. Bei, E.P. George, Acta Mater. 53 (2005) 69–77.
[30] A.H. Clauer, B.A. Wilcox, J.P. Hirth, Acta Metall. 18 (1970) 367–379.
[31] G. Simmons, H. Wang, Single Crystal Elastic Constants and Calculated Aggregate Properties – A Handbook, MIT Press, Cambridge, MA, 1971.
[32] A. Misra, Z.L. Wu, M.T. Kush, R. Gibala, Philos. Mag. A 78 (1998) 533–550.
[33] R.W.K. Honeycombe, Plastic Deformation of Metals, second ed., Edward Arnold, London, 1984.